Conspiracy beliefs and perceptual inference in times of political uncertainty

Salomé Leclercq, Sébastien Szaffarczyk, Pantelis Leptourgos, Pierre Yger, Alexandra Fahkri, Marielle Wathelet, Vincent Bouttier, Sophie Deneve, Renaud Jardri

CONSPIRACY BELIEFS AND PERCEPTUAL INFERENCE IN TIMES OF POLITICAL UNCERTAINTY

AUTHORS

Salomé LECLERCQ[1*], Sébastien SZAFFARCZYK[1], Pantelis LEPTOURGOS[1], Pierre YGER[1], Alexandra FAKHRI[2], Marielle WATHELET[1], Vincent BOUTTIER[1,3], Sophie DENÈVE[3], Renaud JARDRI[1,3*]

1. Lille University, INSERM U1172, CHU Lille, Lille Neuroscience & Cognition Centre, CURE platform, Fontan Hospital, 59000 Lille, France
2. Otto-von-Guericke Universität Magdeburg, Germany
3. Ecole Normale Supérieure, Institut de Sciences Cognitives, LNC, INSERM U-960, Paris F-75005, France

Correspondence to : salome.leclercq@univ-lille.fr ; renaud.jardri@univ-lille.fr

ABSTRACT

Sociopolitical crises causing uncertainty have accumulated in recent years, providing fertile ground for the emergence of conspiracy ideations. Computational models constitute valuable tools for understanding the mechanisms at play in the formation and rigidification of these unshakeable beliefs. Here, the *Circular Inference* model was used to capture associations between changes in perceptual inference and the dynamics of conspiracy ideations in times of uncertainty. A bistable perception task and conspiracy belief assessment focused on major sociopolitical events was performed on large populations from three polarized countries. We show that when uncertainty peaks, an overweighting of sensory information is associated with conspiracy ideations. Progressively, this exploration strategy gives way to an exploitation strategy in which increased adherence to conspiracy theories is associated with the amplification of prior information. Overall, the *Circular Inference* model sheds new light on the possible mechanisms underlying the progressive rigidification of conspiracy theories when individuals face highly uncertain situations.

INTRODUCTION

Conspiracy theories (CTs) are appearing with increasing frequency in our modern societies, with criticism of mainstream knowledge and scientific evidence at center stage. CTs are commonly defined as beliefs assuming the existence of a secret group or organization operating maliciously and for its own benefit. Adherence to multiple unrelated CTs that contradict each other is common[1–4], suggesting common underlying mechanisms by which belief in CTs arises.

Interestingly, a first line of research revealed that these rigid beliefs often crystallize around highly polarizing societal or political events[5] and may serve as coping mechanisms for stress and loss of control when uncertainty increases sharply[6–10]. Although CTs can induce widespread misconceptions - as it has been observed during the COVID-19 pandemic - they also constitute intuitive explanations for complex issues (e.g., simple cause-effect relationships), that can meet the need to restore predictability[11] at the cost of suboptimal reasoning.

A second line of research focused on the role of reasoning biases in CT emergence[12–14]. According to this framework, it is thought that conspiracists bias the weight they attribute to certain stimuli to reduce uncertainty[15,16], sometimes leading people to jump to conclusions (JTC) when probabilistic decisions must be made. Conspiracy ideations have also been associated with a more intuitive thinking style[3,14] than the common analytical approach. This tendency toward fast, preconscious and spontaneous processing could be based on specific reality-testing deficits in people endorsing CTs[17].

These results have not always been replicated, leading some authors to wonder whether CTs could mainly be traced back to social constructs[18–20]. However, others suggest that social learning depends on broader associative mechanisms responsible for the detection of predictive relationships in every natural domain[21]; thus, Bayesian methods could be a complementary approach to addressing the existing link between CTs and uncertainty. This framework assumes that cognitive and perceptual factors are rooted in a common probabilistic mechanism[22]. Surprisingly, only a few attempts have been made to investigate the potential links between perceptual inference and conspiracy ideations in a controlled experimental setting.

Some results from the CT literature appear compatible with a probabilistic formalism. Dagnall and colleagues[23] explored the link between CTs and a wide range of cognitive-perceptual factors. They showed that such factors, including hallucination proneness, often conceptualized as false inferences[24], were associated with CTs. Additionally, conspiracy ideations were found to be associated with illusory visual pattern detection[19,25], a phenomenon regularly explored through the prism of Bayesian theory[26].

Very few papers have directly fitted computational models to behavioral data in nonclinical samples with some noticeable exceptions exploring paranoia and/or conspiracy ideations[27,28]. Purely theoretical papers also confirmed that computational approaches could help to better understand the spreading of CTs on simulated or social-media data[29,30]. Crucially, a more personalized computational lens[31], and a study of CTs in their ecological environment[32] seem required to decipher the respective contributions of sociopolitical factors and information weighting in CTs' emergence.

Thus, combining the strength of normative and ecological research during uncertain societal crises appears necessary to establish a bridge between CT and inference quantification. In the present paper, we referred to *Circular inference* (CI), a Bayesian framework that has proven effective in capturing both perceptual suboptimality in nonclinical populations[33] and JTC in patients with psychosis[34,35]. We hypothesized that by fitting the CI model to a simple bistable task (which maximizes ambiguity at the perceptual level), we could benefit from an ideal setup to challenge the potential links between (i) the inferential mechanisms at play under conditions of extreme uncertainty, and (ii) the dynamics of conspiracy ideations in large populations exposed to natural sociopolitical stress.

RESULTS

Measuring multilevel inference before and after stressful political events

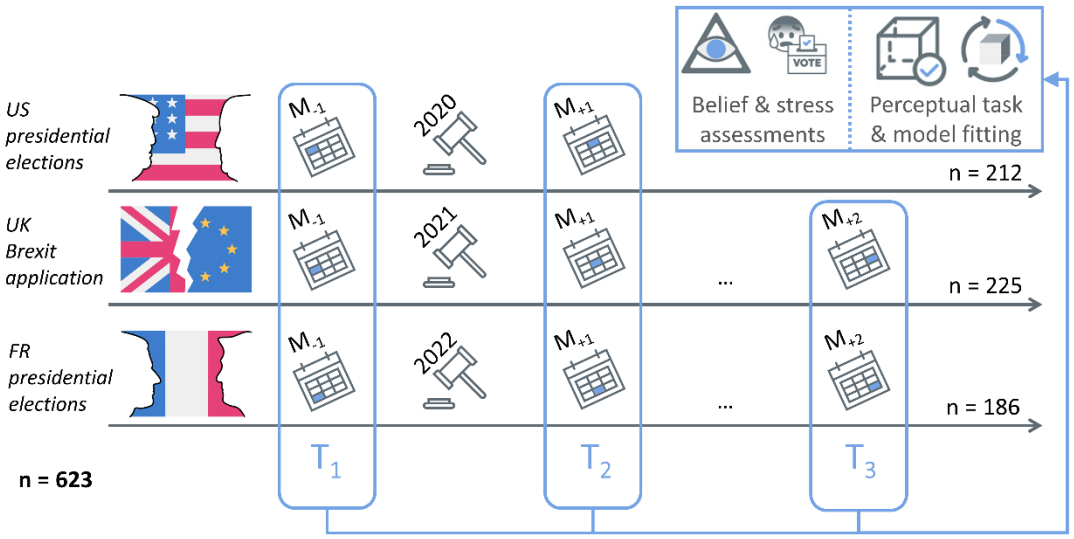

FIGURE 1. A repeated-measures design framing stressful political events in 3 different countries. Conspiracy ideations, political distress and perceptual stability were measured in the same participants (n = 623) via an online procedure, before and after the occurrence of a polarizing political event in three Western countries (M stands for month): the 2020 presidential election in the *United States of America* (n = 212, US), BREXIT implementation in the *United Kingdom* (n = 225, UK) and the 2022 presidential elections in *France* (n = 186, FR). We used T1 and T2 measures in the main model, while T3 was used in control analyses (see ***Supplementary Material section: Controlling for experimental design biases***).

Because we assumed that periods of great sociopolitical uncertainty lead to significant increases in individual levels of distress and favor inferential biases such as conspiracy endorsements, we explored rigid beliefs and perceptual stability around polarizing political events in three independent Western countries (see **Fig. 1**): the *United States of America* (US, 2020 presidential elections), the *United Kingdom* (UK, 2021 BREXIT implementation) and *France* (FR, 2022 presidential elections). At each time point, healthy participants were instructed to rate their level of distress related to the ongoing event in their own country (later referred to as ***political distress***, see ***Methods*** and ***Supplementary Material section: Self-reported measures***).

TABLE 1. Description of the populations at baseline.

	Sex (F /M)	**Age** (y.o.)	**Education**	**pol. distress**	**GCB**	**stability**
Whole Sample (n = 623)	310 / 311	33.0 ± 10.9	5.64 ± 1.41	5.07 ± 3.48	33.8 ± 13.3	.572 ± .178
US (n = 212)	119 / 106	30.4 ± 9.83	5.22 ± 1.43	4.60 ± 3.88	37.7 ± 13.9	.585 ± .173
UK (n = 225)	98 / 112	38.2 ± 10.7	5.52 ± 1.44	5.69 ± 3.32	33.3 ± 13.7	.566 ± .178
FR (n = 186)	93 / 93	29.8 ± 9.90	6.25 ± 1.12	4.87 ± 3.07	30.0 ± 11	.565 ± .183

US: United States of America; UK: United Kingdom; FR: France; F/M: female or male; y.o., years old; Education levels are provided according to the International Standard Classification of Education (ISCED); pol. distress: political distress; GCB: Generic Conspiracist Beliefs Scale; stability: fitted stability score (see *Methods section: Judgment criterion*). The sex-ratio did not differ across samples (X^2 = 1.68, p = .431). UK participants were significantly older (F(2.408) = 44.255, p < 0.001, $\eta^2 = 1.29e^{-19}$) and FR participants reached a higher educational attainment (F(2.411) = 35.458, p < 0.001, $\eta^2 = 3.76e^{-13}$) than the other samples. UK participants demonstrated a higher level of political distress (F(2.408) = 5.8388, p = .00316, $\eta^2 = 2.82e^{-3}$), while stability was consistent across samples (F(2.405) = 0.81828, p = .442).

Necker cube experiment

At each time point, the 623 enrolled participants performed an online bistable perception task based on the Necker cube (NC). The interpretation of the two-dimensional NC projected from a three-dimensional space naturally alternates between two possible configurations: a *seen from above* (SFA), or a *seen from below* (SFB) cube (**Fig. 2a**). A perceptual ***stability score***, ranging from 0 to 1, was estimated at the participant level. This score corresponds to the probability of switching from one interpretation to the other (0 means total instability, while 1 reflects a perceptive rigidity where the participant only sees one interpretation of the two, see the ***Methods*** section). Assuming a universal mechanism at the roots of belief formation, we merged the 3 samples after ensuring their comparability in terms of perceptual stability at baseline (**Table.1, Fig. 2b-c;** see also ***Supplementary Material section: Controlling for experimental design biases***). Importantly, perceptual stability was tested for *in lab/online* within-subject reproducibility on a pilot independent sample before running the final online experiment (**Fig. 2d-e**). We also ensured that dynamic changes in stability between the different time points were not due to a simple training effect between the sessions (see ***Supplementary Material section: Controlling for experimental design biases***).

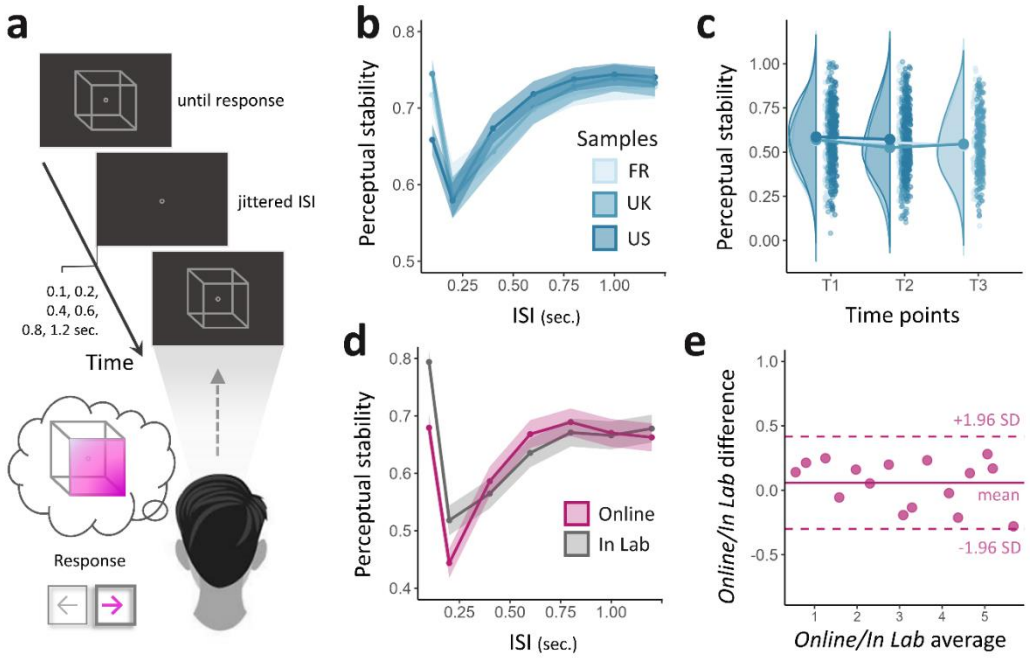

FIGURE 2. The Necker cube (NC) task: procedure and validity. (a) The experimental procedure consisted of serial NC presentations. Each trial was decomposed into three steps (see *Methods* section). After a fixation cross of pseudorandomized duration (ISI) (1), the Necker cube was presented (2) until participants reported their interpretation of the stimulus: 'seen from above' (SFA) or 'seen from below' (SFB), using the right or left arrow of their keyboard, respectively (3). **(b)** Perceptual stability as a function of the interstimulus interval (ISI) for each national sample. US (United States of America, mean Stability Score= .587, s.d.= .172), UK (United Kingdom, mean Stability Score= .570, s.d.= .176) and FR (France, mean Stability Score= .565, s.d.= .1472). **(c)** Averaged stability scores at each time point for the three national samples. **(d)** Perceptual stability as a function of ISI, for online (mean stability score= .441, s.d.= .190) and in-lab methods (mean stability score= .500, s.d.= .140). **(e)** Bland-Altman plot of the agreement between online and in-lab methods comparing stability scores obtained in each condition for the same participants (n = 16). The x axis represents the average scores of the two methods. The y axis represents the mean difference between online and in-lab stability scores. The limits of agreements (LoA, pink dotted lines) are defined as the mean difference computed on all participants (pink line) ± 1.96 s.d., and each dot represents a participant. As all participants are included in the LoA, the methods are considered to be in agreement and may be used interchangeably.

Conspiracy adherence measures

The participants were instructed to self-rate their level of adherence to CTs, completing the *Generic Conspiracist Beliefs Scale* (**GCB**, see *Methods* section) at each time step. Replicating previous findings, we showed that conspiracy ideations were not normally distributed across the tested participants (**W = .954 ; p = .440e^{-12}**, **Fig. 3a, Fig. S1a**), suggesting that only a subpart of the general population commonly endorses such beliefs. The distribution of the total GCB scores differed across the three samples (**χ^2 = 31.5, p <.001, η^2 = .348e^{-07}**) despite a similar pattern across subscales (**Fig. S1a-b, Table S1**), notably demonstrating a common preoccupation for information control.

Looking more precisely at the sociodemographic features associated with conspiracy endorsement, we replicated previous findings from the literature (see ***Supplementary Material section: Sociodemographic features of conspiracy theories***), notably showing that despite an absence of a link with the sex of participants (**Fig. 3b**), GCB scores significantly differed as a function of age (**F(2,620) = 3.10, p = .046, η^2 = .039**, **Fig. 3c**) or education (**F(2,620) = 13.5, p <.001, η^2 = .395e^{-05}**, **Fig. 3d**). Thus, we retained those variables as covariates for later analyses.

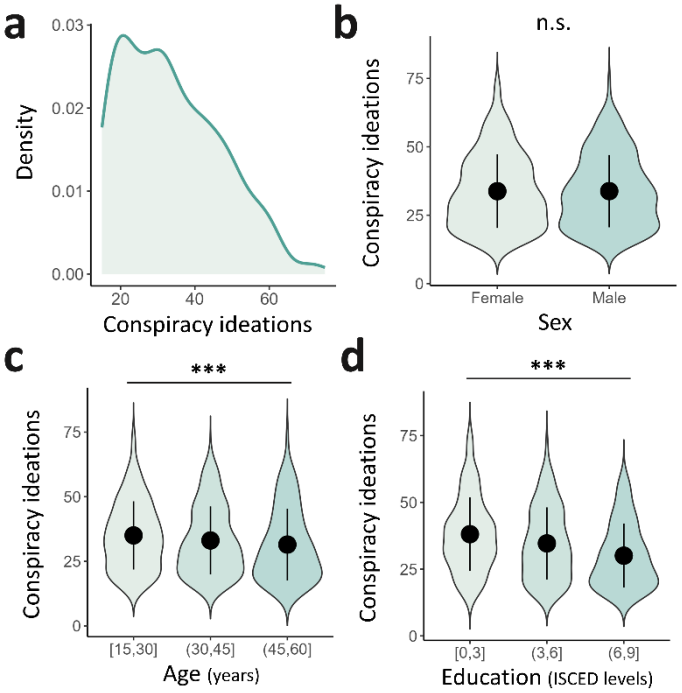

FIGURE 3. Sociodemographic features associated with conspiracy theories at baseline. **(a)** Left-skewed distribution of GCB scores across the entire international sample (N = 623). **(b)** Mean conspiracy scores in females (n = 310, mean = 33.8, s.d. = 13.5) and males (n = 312, mean = 33.8, s.d. =13.2). The between groups difference was not significant. **(c)** Mean conspiracy scores according to age level. *Young* participants (n = 310, age = [18;30]) displayed higher GCB scores (mean = 35, s.d. = 13.2) than the *adults* (n = 210, age = (30;45], mean = 33.1, s.d. = 13.2) and older *adults* (n = 103, age = (45;60], mean = 31.5, s.d. = 13.8). **(d)** Mean conspiracy scores according to educational attainment levels. *The low education* group (n = 86, ISCED = [0;3]) scored significantly higher on GCB (mean = 38.2, s.d. = 13.7) than the *medium education* (n = 363, ISCED = [3;6], mean = 34.7, s.d. = 13.5) and the *high education* groups (n = 179, ISCED = [6;9], mean = 30, s.d. = 12).

Stress correlates at baseline

We assume that some participants might adopt information-processing strategies that can reduce the uncertainty induced by the framed political event. Notably, we expect that the search for stability would translate into high levels of confidence measurable at different levels of processing, from perception to conspiracy beliefs. Since belief in CTs has been proposed to be a coping strategy able to reduce the stress elicited by uncertainty, we also expect an association between great levels of confidence and low levels of distress. We first checked for associations between political distress at baseline (i.e., when uncertainty peaked) and: (i) perceptual stability on the one hand, and (ii) conspiracy endorsement on the other hand (**Fig. 4a**). Political distress was found to be negatively linked

with both levels of inference (**p = .028, ρ = -.120** and **p = .007, ρ = -.094** respectively). We further confirmed these findings by splitting the sample into two subsamples according to stress: (i) a 'low stress' (**LS**) and (ii) a 'high stress' group (**HS**). Comparing these two groups at baseline, we confirmed a significant difference in both stability (**U = 41385, p = .002, Cohen's *d*= .140**) and GCB scores (**U = 43411, p = .023, Cohen's *d* = .110**), such as the LS group scored higher in both (**Fig. 4d-e**).

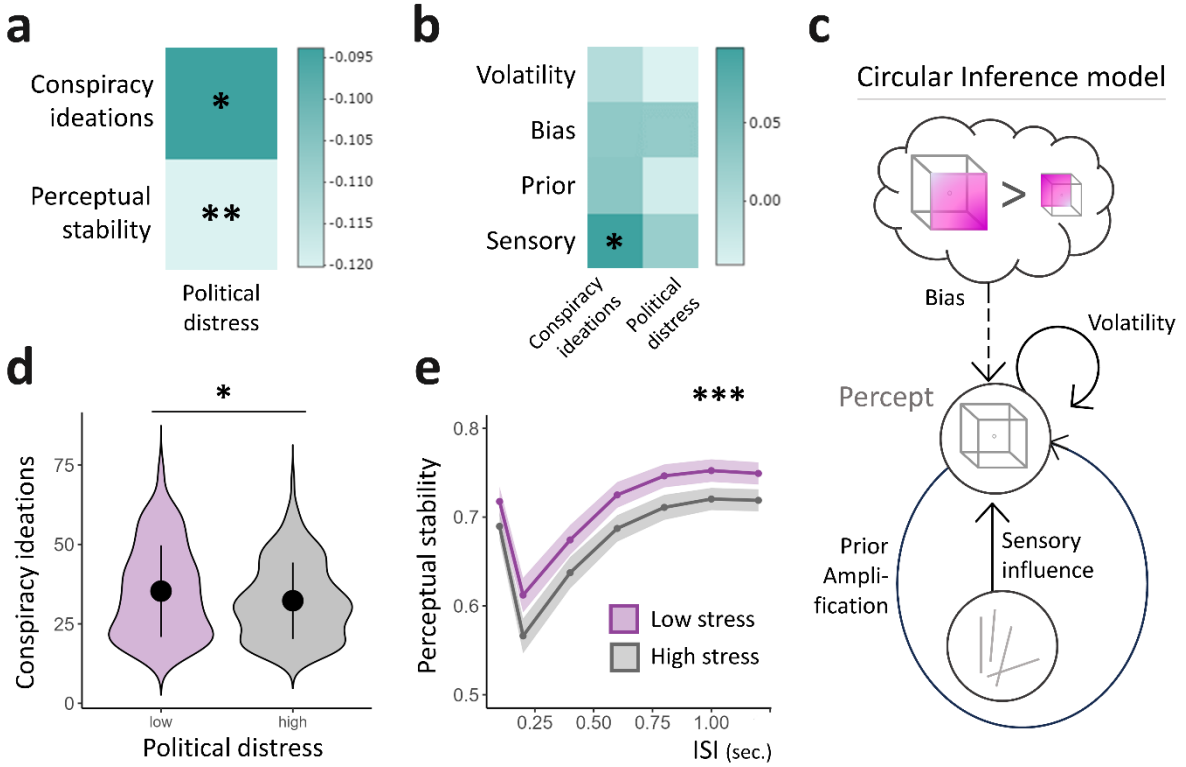

FIGURE 4. Cognitive and perceptual inference correlates at baseline.

(a) Heatmap depicting the strength of associations at baseline between political distress, conspiracy ideations measured with the *Generic Conspiracist Beliefs Scale* (GCB) and perceptual stability (Pearson's correlations, corrected for multiple comparisons using the *false discovery rate* method, FDR). Political distress was negatively associated with GCB **(ρ = -.094)** and perceptual stability scores **(ρ = -.120)**. **(b)** Heatmap illustrating the strength of associations at baseline between GCB scores, political distress and Circular Inference parameters (sensory weight (w), prior amplification (a), bias ($r_{on} - r_{off}$) and volatility (r_{on})). Pearson's correlations were corrected for multiple comparisons using FDR. GCB scores were significantly associated with sensory overweighting **(ρ = .098)**. **(c)** The Circular Inference (CI) model relies on 4 parameters: the overall sensory gain (sensory, w), the descending loops (prior, a), the transition rate (volatility, r_{on}) and the configuration preference (bias, ($r_{on} - r_{off}$)) (see *Methods*). **(d)** Mean conspiracy scores in the *low stress* (LS) group (n = 310, mean political distress = 2.10, s.d. = 2.06; mean conspiracy score = 35.3, s.d.= 14.4) and *high stress* (HS) group (n = 313, mean political distress = 8.01, s.d.= 1.58; mean conspiracy score = 32.3; s.d.= 12.0). GCB scores were significantly higher in the LS group (**Cohen's *d* = .110**). **(e)** Perceptual stability plotted as a function of inter-stimulus-interval (ISI) in LS (mean stability score = .597; s.d.= .176) and HS (stability score = .548; s.d.= .177) groups. Perceptual processing was found significantly more rigid in the LS group than in the HS group (**Cohen's *d* = .140**;). * stands for p<.05, ** for p<.01 and *** for p<.001.

We then looked at the influence of age, education, political distress and perceptual stability on GCB scores (**F(4,618) = 11.1, p <.001, adjusted R^2 = .061**). Again, we found that age (estimate = -.125, **p = .009**), and education (estimate = -1.88, **p <.001**) were significantly associated with CTs, further confirming that political distress (estimate = -.396, **p = .009**) had a significant impact on conspiracy endorsement, even after controlling for those sociodemographic factors.

Fitting the Circular Inference Model

Because we conceptualized perception as an inferential process, we also fitted the *Circular Inference* model to the Necker cube data (**Fig. 4c**). We have previously found that CI can explain NC data better than other pure Bayesian models[33]. This approach allowed us to quantify four model parameters contributing to the perceptual decision: sensory weight, prior amplification, bias, and volatility. We checked whether these CI parameters could capture the effects of political distress and conspiracy adherence. Sensory weight was the only parameter positively associated with GCB scores at baseline (**p = .030, ρ = .098, Fig. 4b**), supporting the idea that participants more prone to CTs at baseline rely more on sensory evidence when asked to make a decision in a highly ambiguous environment. We confirmed this GCB-sensory weight association (**estimate = 1.20, p = .051**) even after controlling for the effects of age, education and political distress (**F(4,618) = 11.86, p <.001, adjusted R^2 = .065**).

Measured changes after political event resolution

We then assessed changes in political distress, conspiracy ideations and perceptual stability over time (**Table.2**). We confirmed an overall stress reduction at T2 compared to that at baseline (**W = 100834, p <.001, Cohen's *d*= -.250** ; **Fig. 5a**), despite some heterogeneity in the participants. Meanwhile, GCB scores significantly increased (**W = 73048, p = .017, Cohen's *d* = .068**), while stability scores decreased (**W = 114427, p <.001, Cohen's *d* = -.139**) – this tendency toward destabilization was observed in each national sample (see also **Fig. S3**).

TABLE 2. Population description at each time-step: scores, and CI parameters.

	pol. distress	GCB	stability	sensory	prior	bias	volatility
T1	5.35 ± 3.33	33.78 ± 13.33	.57 ± .18	1.70 ± .85	1.85 ± .91	.59 ± .07	-2.04 ± 1.50
T2	4.54 ± 3.16	34.70 ± 13.56	.55 ± .18	1.65 ± .85	1.86 ± .93	.59 ± .06	-2.20 ± 1.40

Pol. distress: political distress; GCB: Generic Conspiracist Beliefs Scale; stability: estimated stability score (see also *Methods section: Judgment criterion*); Sensory: sensory overweighting (w); Prior: prior amplification (α).

To account for the heterogeneity in stress evolution, we split the sample into two subgroups according to their trajectories: a first subsample with decreasing stress (**Dec**, n=330) and a second subsample with increased stress between T1 and T2 (**Inc**, n=227; **Fig. 5b**). Considering that the Dec group should have adopted the most efficient coping strategies, we checked how the CI parameters and degree of conspiracy ideations changed over the same period in these two subsamples (**Table.S3**).

A delta measure for each CI parameter was computed (parameter value at retest minus value at baseline), such as a positive delta indicated a gain in the parameter value, while a negative delta reflected a decrease in this parameter. The Dec group showed increased reliance on prior information in the bistable task between T1 and T2 (mean ΔPrior=.0811, s.d=1.11), while the Inc group showed decreased use of priors in the same period (mean ΔPrior=-.121, s.d.=1.14). This difference was statistically significant (**t(460.65) = 2.07, p = .039, Cohen's *d* = .180** ; **Fig. 5c-left**). We found no differences in the 3 other CI parameters (**Fig. S3**).

FIGURE 5. Computational and cognitive features associated with changes in political distress over time.

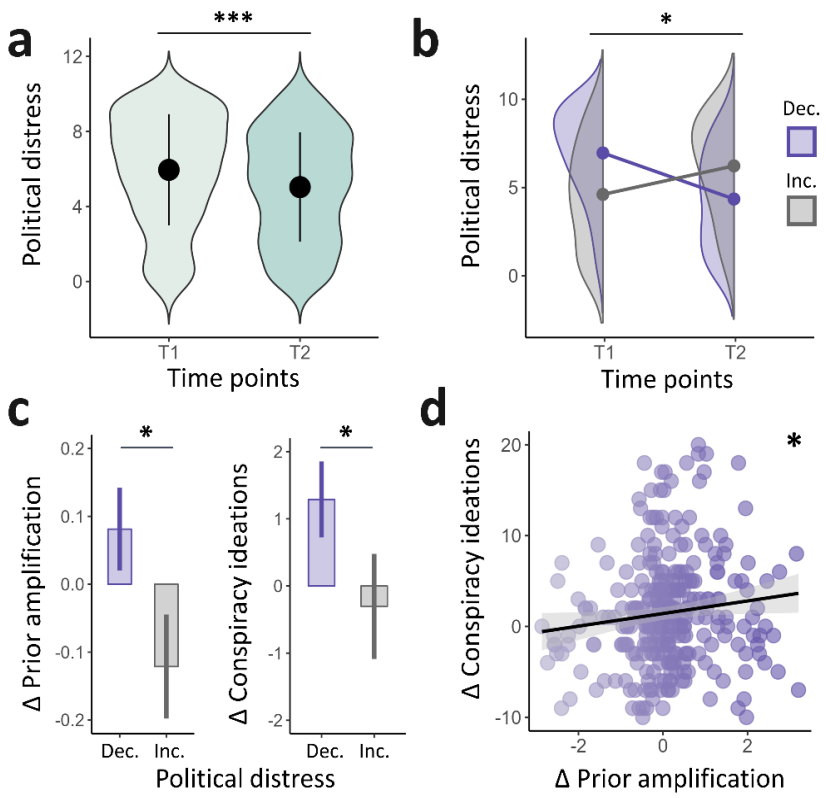

(a) Illustration of political distress scores over testing sessions. Political distress decreased between baseline (T1, mean political distress = 5.35, s.d. = 3.33) and retest (T2, mean political distress = 4.54, s.d. = 3.16; **Cohen's *d* = -.250**). **(b)** Political distress over time according to stress trajectories. Some participants showed decreased political distress after uncertainty resolution (Dec, n = 330, mean Δpolitical distress = -2.78, s.d. = 2.45), while another subsample showed increased stress (Inc, n = 220, mean Δpolitical distress = 2.01, s.d. = 2.14). **(c)** Left: Illustration of the evolution of prior amplification (ΔPrior) over time for the 'Dec' (mean = .081, s.d. = 1.11) and 'Inc' (mean = -.121, s.d. = 1.14) groups. The intergroup difference was significant (**Cohen's *d* = .180**). Right: Evolution of conspiracy ideations (ΔConspiracy ideations) over time for the 'Dec' (mean = 1.29, s.d. = 10.3) and 'Inc' (mean = -.305, s.d. = 11.6) groups. The intergroup difference was significant (**Cohen's *d* = .145**) **(d)** Scatter plot showing the correlation between ΔPrior and ΔConspiracy ideations in the 'Dec' group (p = .035, ρ = .116; Spearman correlation, **ρ = .116**). * indicates p<.05, *** indicates p<.001.

We also computed a composite ΔGCB score corresponding to GCB at retest minus GCB at baseline, such that a positive delta corresponded to an increase in conspiracy adherence while a negative delta resulted in a decrease. We observed a trend for conspiracy strengthening in participants with decreased stress in comparison with that observed in the rest of the sample (t(429.52)=1.65, p = .099, Cohen's *d* = .145). Because conspiracy ideations were proposed to act as a coping mechanism when facing uncertainty, we next ran an oriented test to confront that hypothesis which reached significance (**t(429.52)=1.65, p = .050, Cohen's *d* = 0.145 ; Fig. 5c-right**). This finding supports a gain in the GCB score for the Dec group compared to the Inc group. To confirm the idea that the GCB score increase was directly associated with an increase in Prior in the Dec group, we compared ΔPrior and ΔGCB in this specific subsample; these measures were found to be positively associated (**p = .035, ρ = .116, Fig. 5d**).

DISCUSSION

A surge in CTs has been observed in recent years, and CTs have been proposed to act as coping strategies for the stress and perceived lack of control generated by global uncertainty[6–10]. CTs offer intuitive and easy-to-understand explanations to unsolved problems[36]. Links have already been established between conspiracy endorsement and some inference biases[3,12–14]. However, very few studies have primarily focused on low-level perceptual aspects of conspiracy[19,20,23,25], and limited efforts have been made to delve into the potential mechanisms of information processing that may convey such associations.

To address these concerns, we combined online assessments of bistable perception in large international samples with Bayesian modeling. This approach allowed us to quantify perceptual inference mechanisms and to test their links with conspiracy ideations during periods of great sociopolitical uncertainty. We were able to capture the rigidification of conspiracy beliefs in nonclinical populations. Specifically, using the Circular Inference (CI) model, we highlighted a significant association between conspiracy endorsement and the overweighting of sensory information when ambiguity reaches a climax, later followed by a selective increase in prior reliance in those who subsequently decreased their stress levels.

Several attempts at modeling the features of conspiracy beliefs can be found in the literature. However, most of these models have either focused on the network scale[37] or remained purely theoretical, without experimental testing[31]. Recent findings highlighted the added value of a computational framework to account for the emergence of rigid beliefs during the COVID-19 pandemic[27] and the protective aspect of CTs against distress in a social context[38]. These studies used high-level cognitive tasks and mainly focused on paranoia, a condition sharing some phenomenological features with CTs but also considered significantly different[39], further justifying specific explorations. The quantitative approach proposed in the present work nicely completes these initiatives, adding the testing of low-level inference, together to measurements of conspiracy beliefs' emergence and rigidification.

Here, we provide the first evidence for an association between sensory information overweighting in ambiguous contexts and a high level of conspiracy endorsement. This finding suggests that when uncertainty peaks, a subpart of the population, more vulnerable to stress, is prone to embracing conspiracy explanations based on intuitive reasoning. Motivated by the need to cope with uncertainty, these participants first adopt an "exploration" strategy, seeking explanations in their direct environment to make their perceptual decisions. Interestingly, such a mechanism accounts for perceptual and inferential biases previously found to be associated with conspiracy ideations, such as illusory pattern detection[19,20,25], intuitive thinking[40,41] and the JTC phenomenon[15,16].

We also explored the dynamic changes in model parameters after stress resolution by using a pre/post design surrounding the political events. We shed light on the association between prior knowledge amplification in perceptual decisions and the enhanced adherence to CTs in those who showed reduced stress level. This finding suggests that some participants coped with uncertainty by embracing conspiracy-oriented explanations, secondarily shifting to an "exploitation" strategy (**Fig. S5**), validating their newly established view and reinforcing their own beliefs. This second mode appears compatible with findings showing confirmation biases (Brotherton, 2015) and reality testing deficits[17] in people with CTs, making these beliefs more resilient to counterevidence.

These results can also be compared with models of the emergence and maintenance of clinical beliefs, such as delusional ideations. Indeed, prior research conceptualized delusion formation as the result of impaired associative learning processes driven by excessive prediction error[42], a framework that was later extended to account for delusion persistence as aberrant reinforcement of previously leaned associations[43]. Our results also add to previous work showing that parametric changes might mimic behaviors observed during the transition to psychosis[44]. It was shown using CI-based simulations that the seminal amplification of sensory information involved in the integration of aberrant causal relationships (during the transition to psychosis) subsequently constituted strong priors proposed as responsible for the stability of delusional contents from one psychotic episode to the next. Both approaches (predictive coding and Bayesian modeling) are congruent with (i) the idea that conspiracy endorsement is associated with the establishment of aberrant causal relations between random events[6], and (ii) that conspiracy could be rooted in the self-reinforcement of previously integrated suboptimal beliefs.

While the endorsement of CTs may serve as an effective short-term coping strategy, it also appears to pave the way for the long-term rigidification of suboptimal beliefs (beliefs that would be computed through mechanisms deviating from Bayes' rule), making it maladaptive for stress-regulation overall. The social implications of gaining a better understanding of this phenomenon are vast. Humankind has experienced repeated periods of heightened uncertainty throughout history, ranging from civilizational collapses or wars to economic crises. In extending the well-established association between political distress and the endorsement of CTs[5], our model also explains the recent rise in extremism and populism observed since the beginning of the XXIst century in a global context of the pandemic, terror attacks and climate change.

We must acknowledge some limitations of this work. First, although significant, some results exhibit small effect-sizes (i.e., Cohen's *d* around 0.2). Of note, small effect-sizes were previously found to still have substantial significance when studies were conducted on large populations[45]. It is also important to remember that small effects were expected because we attempted to capture an association between a low-level inference process (bistable perception) and a more complex cognitive process (conspiracy). These findings still constitute an important proof-of-concept demonstration that the CI model can capture small variations in nonclinical populations' perceptual decisions, paving the way for promising advancements in deepening our understanding of the mechanisms underlying belief rigidification.

A second limitation is that we cannot rule out that some participants may have felt hesitant in honestly reporting their views about CTs, due to the controversy and potential stigma surrounding conspiracy thinking. However, we think that our experimental design offers two advantages in the valid assessment of conspiracy endorsement. First, its online nature ensured anonymity and encouraged freedom of speech, as frequently observed on the internet and digital social media. Second, the joint use of a low-level perceptual task, the NC, provided access to a proxy of inference processing that is rarely prone to social biases, such as interviewer compliance.

A third limitation is the representativity of the sample: we indeed chose to recruit participants from three Western educated countries, known for their high degree of polarization[46]. Although our sample may not represent the world population, we argue that the phenomenon we are investigating follows some universal rules. First, links between sociopolitical uncertainty and the resurgence of conspiracy beliefs have already been observed at various times and locations, dating back to the Roman Empire[47]. Second, while the GCB total scores were distributed differently among our three samples (**Fig. S1a**), their qualitative distribution across GCB subscales followed the same pattern (**Fig.**

S1b). Third, the main results and trends (i.e., sometimes not reaching significance due to the reduced statistical power) appear consistent across the 3 samples when tested separately (**Fig. S2**).

For the same reasons, we focused on the level of distress related to specific political events in the countries where the tests took place. Importantly, we did not consider other types of individual stress levels. Instead, we concentrated on the broader phenomenon of sociopolitical uncertainty.

Overall, this study highlights the potential of the Circular Inference model in examining subtle variations in inference processing associated with high-level cognitive beliefs. This model has already proven effective in accounting for the positive symptoms of schizophrenia[34,35,48] and schizotypal traits[49]; however, this breakthrough opens up new avenues for applying quantitative approaches to dynamically explore subjective beliefs in nonclinical populations. By applying this computational framework, we delved deeper into the mechanisms underlying the emergence and maintenance of conspiracy beliefs, shedding light on their societal impact and providing insights that could be valuable for developing interventions aimed to counter the influence of CTs during highly uncertain periods.

METHODS

Participants

Three independent samples were recruited using the Prolific© web-platform: 212 US citizens, 225 British citizens and 186 French citizens. The same protocol was administered 1 month before and 1 month after a major stressful political event: the 2020 US presidential election, the 2021 UK BREXIT implementation and the 2022 French presidential election (**Fig. 1**). The targeted participants were aged between 18 and 60 and had normal-to-corrected vision. They were from the nationality of the country of interest for each sample and regularly used social media. Th exclusion criteria were a history of psychiatric or neurological disorder, strabismus, or eye surgery. From the initial sample (N = 755), 30 participants were excluded based on failed attentional checks (see ***Supplementary Material section: Controlling for experimental biases***) or very-low reaction times (mean reaction time < 300ms), while 102 were lost longitudinally.

The Prolific© web-platform (https://www.prolific.co/) ensures data privacy following standards of the European and UK data protection law (i.e., General Data Protection Regulation (GDPR), transposed into UK law as the UK GDPR). Participants' sociodemographic characteristics were associated with their respective behavioral data through an anonymous ID randomly assigned at enrollment. The overall online survey complies with French regulations and ethics (*Comité de Protection des Personnes Nord-Ouest IV*).

Apparatus

The protocol was implemented in PsychoPy v.3, exported and hosted online on the Pavlovia.org platform. For the perceptual part of the experiment, participants were instructed to stand in total darkness, approximately 60 cm away from the screen and adjust it to be perpendicular to the floor with their eyes aligned to the fixation cross displayed at the center of the screen. The NC task and the self-reported assessment of beliefs were administered in a randomized order (see also ***Supplementary Material section: Controlling for experimental biases***).

The Necker Cube Task

Stimuli:

Visual stimuli representing Necker cubes (NC) were displayed in the center of a black screen. The stimulus size was standardized across the participants using a matching method based on a standard credit card displayed on the screen that the participant was required to adjust in size before starting the experiment (GitHub link to add).

Procedure:

The block-design of the task was inspired by Mamassian and Goutcher's[50] protocol. During each block, a NC was presented discontinuously. Referring to a forced-choice methodology, we asked participants to report their interpretation of the stimulus using their keyboard each time a new cube appeared on the screen. The cube disappeared after a pseudorandom duration (**ISI** ranging from 0.1 to 1.2 seconds). Each recorded response constituted a trial, and the experiment was divided into 10 blocks of 64 consecutive trials (i.e., 640 NC presentations per run), providing a discontinuous sample

of the participant's perceptual dynamics. A 10-second black screen display separated each block to minimize the influence of the previous block on later responses (**Fig. 2a**).

Participants were instructed to stare at the target located in the middle of the screen to neutralize the potential effects of eye movements. The two possible interpretations of the NC (SFA, SFB) were explicitly mentioned, and subjects were asked to look at the cube passively, without attempting to orient or force their perception. A short training session was performed beforehand to give participants the opportunity to become familiar with the stimulus and the task while ensuring that the instructions were well understood.

Judgment criterion

Various parameters can be used to understand and describe the phenomenon of bistable perception. We chose to focus on **perceptual stability** because we were interested in its dynamical dimension, i.e., how the system could stabilise and destabilise.

Perceptual stability is defined as the probability that a percept persists from one trial to the next. According to Markovian modeling, the current percept (one of the two interpretations SFA or SFB) depends on the previous percept and its updating by sensory observation. This implies a circularity in the integration of information where the percept at time *t* becomes the prior information at time *t+1*. A value was thus assigned to each trial "i": 0 if the response was different from the response to trial "i-1" and 1 if the response to trial "i" was identical to the response to trial "i-1". The average SP was thus calculated for all trials and separately for each interpretation (SP0 and SP1 for SFA and SFB, respectively). Overall, the SP was interpreted as the general probability that the system remains stable from one trial to the next, where 1 corresponds to a system with no perceptual change and 0 to a system governed by maximum instability.

A previously proposed way to assess perceptual stability is by computing stability curves representing SP as a function of different ISI values. Such a curve usually consists of an initial “destabilization” portion corresponding to a drastic drop in perceptual stability, and a “stabilization” portion reaching a “ceiling threshold”, considered a good proxy of perceptual stability (**Fig. 2b,d**). This second portion of the curve was fitted to a reversed exponential function, and we considered the parameter corresponding to the last point of the curve as the **stability score** for each participant.

Self-reported measures

A sociodemographic form and some psychometric assessments were then conducted/collected on the Prolific© platform. Participants specified their age and educational attainment as defined in the *International Standard Classification of Education* (**ISCED**)[51]. The participant demographics are shown in **Table.1**. When Likert or visual analogical scales were used, the cursor was coded to return to the center of the screen after each question to avoid the answer being biased by previous ones. Adherence to CTs was assessed using the 15-item *Generic Conspiracist Beliefs Scale* (**GCB**)[52] and its French translation[53]. The GCB scores and subscores for each sample are shown in **Table.1** and **Table.S1**. Participants were also asked to rate with a 10-point visual analogical scale how distressed they were regarding the target event in their country (**political distress**). The precise questions used are shown in the **Supplementary Material section: Self-reported measures**.

Data Analysis and Statistics

Characteristics of conspiracy adherence

The normality of the distributions was tested using the Shapiro-Wilk test. If nonnormally distributed, further analyses were run using nonparametric statistics. Notably, we compared GCB scores between the three US-UK-FR samples using a Kruskal-Wallis test. We compared GCB scores between males and females using a Mann-Whitney test, while GCB scores across ISCED levels of education and across different age levels were compared using Welch ANOVAs.

The correlates of stress at baseline

We conducted a series of model-free analyses to confirm the association between political distress, stability score, and GCB. Again, due to the nonnormal distribution of the GCB scores, we referred to Spearman rank correlations to explore linear associations, corrected for multiple comparisons based on the *false discovery rate* (FDR) method. These analyses were conducted on the whole sample, and on subsamples generated through a median split on the political distress score: the 'low stress' (**LS**, n=310) and 'high stress' (**HS**, n=313) subgroups. We used Mann-Whitney tests to assess the difference between these two subgroups regarding stability scores or GCB scores. We also used a linear regression model to confirm the association between political distress and GCB, adding age and education level as covariates to control for the effect of these sociodemographic factors.

Model fitting

To better understand the association between conspiracy theories and stress, we fitted a dynamical *Circular Inference* model (CI) to the data (for more details, see [33]). Applied to the NC task, CI describes the process through which participants combine prior expectations about the visual appearance of three-dimensional (3D) objects and (illusory) depth cues to compute a 3D interpretation of the two-dimensional (2D) NC : seen from above (SFA) or seen from below (SFB). Belief updating in CI can be formalized as follows:

$$\frac{dL}{dt} = -\Phi(L) + aL + wS$$

This equation describes how the posterior belief about the ambiguous figure L changes over time (positive/negative L corresponds to SFA/SFB beliefs), under the influence of 3 driving "forces": dynamics ($\Phi(L)$), descending loops (aL) and sensory noise (wS).

Function $\Phi()$ describes the (Markovian) dynamics of the system and is equivalent to a leak term. It captures the intuition that in the real-world, objects are not eternal and can appear, disappear or change abruptly. Markovian temporal statistics can be reduced to 2 parameters, r_{on} and r_{off} (corresponding to the probability of switching from SFB to SFA and from SFA to SFB respectively). This term pushes L toward its prior value ($\log(\frac{r_{on}}{r_{off}})$). By making r_{on} greater than r_{off}, we can implement an implicit SFA bias.

The second term describes the auto-amplification of priors due to descending loops (parameter a). According to CI, prior information can be reverberated and counted several times[54]. This overcounting of priors is akin to a positive feedback that strengthens and stabilizes currently held perceptual beliefs, resulting in bistable perception[33].

Finally, the third term describes the sensory noise that drives switches between the 2 interpretations. For simplicity, we assume that S is sampled from a normal distribution with 0 mean and variance equal to 1. Furthermore, w is a free parameter representing the overall sensory weight

(sensory weight and climbing loops are mathematically indistinguishable, so they are both included in w).

In summary, this model of perceptual dynamics can be reduced to 4 free parameters: the overall gain of sensory inputs w (sensory), the descending loops a (prior), the transition rate r_{on} (volatility) and the bias ($r_{on} - r_{off}$).

Changes after political event resolution

We assessed the evolution of political distress, stability scores and GCB scores over time using Wilcoxon signed-rank tests for repeated measures. We then split our sample into two groups: **Dec** and **Inc** comprising individuals who showed decreased or increased stress, respectively, between the two time points. We computed a delta measure for each parameter that corresponded to the parameter's value at retest minus that at baseline. A positive value indicated a gain in the parameter, while a negative value indicated a decrease. Due to the normal shape of distributions in these composite scores and our sample size, we referred to Welch tests for group comparisons.

The same procedure was used to compare the two groups regarding the gain in GCB (ΔGCB). We successively performed a two-tailed Welch's test, followed by Welch's test for the oriented hypothesis that the **Dec** subsample would significantly increase its GCB score compared with the **Inc** subsample. Finally, a Pearson correlation test was used to check for an association between ΔAlpha and ΔGCB in the **Dec** subgroup.

REFERENCES

1. Goertzel, T. Belief in Conspiracy Theories. *Polit. Psychol.* **15**, 731–742 (1994).
2. Swami, V. *et al.* Conspiracist ideation in Britain and Austria: evidence of a monological belief system and associations between individual psychological differences and real-world and fictitious conspiracy theories. *Br. J. Psychol. Lond. Engl. 1953* **102**, 443–463 (2011).
3. Drinkwater, K., Dagnall, N. & Parker, A. Reality testing, conspiracy theories and paranormal beliefs. *J. Parapsychol.* **76**, 57–77 (2012).
4. Wood, M. J., Douglas, K. M. & Sutton, R. M. Dead and Alive: Beliefs in Contradictory Conspiracy Theories. *Soc. Psychol. Personal. Sci.* **3**, 767–773 (2012).
5. van Prooijen, J.-W. & Douglas, K. M. Conspiracy theories as part of history: The role of societal crisis situations. *Mem. Stud.* **10**, 323–333 (2017).
6. Whitson, J. A. & Galinsky, A. D. Lacking Control Increases Illusory Pattern Perception. *Science* **322**, 115–117 (2008).
7. Sullivan, D., Landau, M. J. & Rothschild, Z. K. An existential function of enemyship: Evidence that people attribute influence to personal and political enemies to compensate for threats to control. *J. Pers. Soc. Psychol.* **98**, 434–449 (2010).
8. van Prooijen, J.-W. & Acker, M. The Influence of Control on Belief in Conspiracy Theories: Conceptual and Applied Extensions. *Appl. Cogn. Psychol.* **29**, 753–761 (2015).
9. Dow, B. J., Menon, T., Wang, C. S. & Whitson, J. A. Sense of control and conspiracy perceptions: Generative directions on a well-worn path. *Curr. Opin. Psychol.* **47**, 101389 (2022).
10. Farias, J. & Pilati, R. COVID-19 as an undesirable political issue: Conspiracy beliefs and intolerance of uncertainty predict adhesion to prevention measures. *Curr. Psychol. N. B. NJ* **42**, 209–219 (2023).
11. Douglas, K. M. *et al.* Understanding Conspiracy Theories. *Polit. Psychol.* **40**, 3–35 (2019).
12. Wycha, N. It's a Conspiracy: Motivated Reasoning and Conspiracy Ideation in the Rejection of Climate Change. *Electron. Theses Diss.* (2015).
13. Brotherton, R. & French, C. C. Intention seekers: conspiracist ideation and biased attributions of intentionality. *PloS One* **10**, e0124125 (2015).
14. Georgiou, N., Delfabbro, P. & Balzan, R. Conspiracy theory beliefs, scientific reasoning and the analytical thinking paradox. *Appl. Cogn. Psychol.* **35**, 1523–1534 (2021).
15. Pytlik, N., Soll, D. & Mehl, S. Thinking Preferences and Conspiracy Belief: Intuitive Thinking and the Jumping to Conclusions-Bias as a Basis for the Belief in Conspiracy Theories. *Front. Psychiatry* **11**, 568942 (2020).
16. Kabengele, M.-C., Gollwitzer, P. M. & Keller, L. Conspiracy Beliefs and Jumping to Conclusions. Preprint at https://doi.org/10.31234/osf.io/63apz (2023).
17. Lewandowsky, S., Gignac, G. E. & Oberauer, K. The Role of Conspiracist Ideation and Worldviews in Predicting Rejection of Science. *PLOS ONE* **8**, e75637 (2013).
18. Raihani, N. J. & Bell, V. An evolutionary perspective on paranoia. *Nat. Hum. Behav.* **3**, 114–121 (2019).
19. Müller, P. & Hartmann, M. Linking paranormal and conspiracy beliefs to illusory pattern perception through signal detection theory. *Sci. Rep.* **13**, 9739 (2023).
20. Hartmann, M. & Müller, P. Illusory perception of visual patterns in pure noise is associated with COVID-19 conspiracy beliefs. *-Percept.* **14**, 204166952211447 (2023).
21. Heyes, C. New thinking: the evolution of human cognition. *Philos. Trans. R. Soc. B Biol. Sci.* **367**, 2091–2096 (2012).
22. Helmholtz, H. von. Concerning the perceptions in general, 1867. in *Readings in the history of psychology* 214–230 (Appleton-Century-Crofts, 1948). doi:10.1037/11304-027.
23. Dagnall, N., Drinkwater, K., Parker, A., Denovan, A. & Parton, M. Conspiracy theory and cognitive style: a worldview. *Front. Psychol.* **6**, (2015).
24. Fletcher, P. C. & Frith, C. D. Perceiving is believing: a Bayesian approach to explaining the positive symptoms of schizophrenia. *Nat. Rev. Neurosci.* **10**, 48–58 (2009).
25. van Prooijen, J., Douglas, K. M. & De Inocencio, C. Connecting the dots: Illusory pattern perception predicts belief in conspiracies and the supernatural. *Eur. J. Soc. Psychol.* **48**, 320–335 (2018).
26. Geisler, W. S. & Kersten, D. Illusions, perception and Bayes. *Nat. Neurosci.* **5**, 508–510 (2002).
27. Suthaharan, P. *et al.* Paranoia and belief updating during the COVID-19 crisis. *Nat. Hum. Behav.* **5**, 1190–1202 (2021).
28. Barnby, J. M., Mehta, M. A. & Moutoussis, M. The computational relationship between reinforcement learning, social inference, and paranoia. *PL O Comput. Biol.* **18**, (2022).

29. Cook, J. & Lewandowsky, S. Rational Irrationality: Modeling Climate Change Belief Polarization Using Bayesian Networks. *Top. Cogn. Sci.* **8**, 160–179 (2016).
30. Madsen, J. K., Bailey, R. & Pilditch, T. D. Growing a Bayesian Conspiracy Theorist: An Agent-Based Model. *In: Gunzelmann, G and Howes, A and Tenbrink, T and Davelaar, E, (eds.) Proceedings of the 39th Annual Meetng of the Cognitive Science Society (CogSci 2017). (pp. pp. 2657-2662). Cognitive Science Society (2017)* vol. 39 2657–2662 https://mindmodeling.org/cogsci2017/papers/0503/index.html (2017).
31. Rigoli, F. Deconstructing the Conspiratorial Mind: the Computational Logic Behind Conspiracy Theories. *Rev. Philos. Psychol.* 1–18 (2022) doi:10.1007/s13164-022-00657-7.
32. Stojanov, A., Bering, J. M. & Halberstadt, J. Perceived lack of control and conspiracy theory beliefs in the wake of political strife and natural disaster. *Psihologija* **55**, 149–168 (2022).
33. Leptourgos, P., Notredame, C.-E., Eck, M., Jardri, R. & Denève, S. Circular inference in bistable perception. *J. Vis.* **20**, 12–12 (2020).
34. Jardri, R., Duverne, S., Litvinova, A. S. & Denève, S. Experimental evidence for circular inference in schizophrenia. *Nat. Commun.* **8**, 14218 (2017).
35. Simonsen, A. *et al.* Taking others into account: combining directly experienced and indirect information in schizophrenia. *Brain J. Neurol.* **144**, 1603–1614 (2021).
36. van Prooijen, J.-W. Why Education Predicts Decreased Belief in Conspiracy Theories. *Appl. Cogn. Psychol.* **31**, 50–58 (2017).
37. Peruzzi, A., Zollo, F., Schmidt, A. L. & Quattrociocchi, W. From confirmation bias to echo-chambers: a data-driven approach. *Sociol. E Polit. SOCIALI* (2019) doi:10.3280/SP2018-003004.
38. Suthaharan, P. & Corlett, P. R. Assumed shared belief about conspiracy theories in social networks protects paranoid individuals against distress. *Sci. Rep.* **13**, 6084 (2023).
39. Greenburgh, A. & Raihani, N. J. Paranoia and conspiracy thinking. *Curr. Opin. Psychol.* **47**, 101362 (2022).
40. Swami, V., Voracek, M., Stieger, S., Tran, U. S. & Furnham, A. Analytic thinking reduces belief in conspiracy theories. *Cognition* **133**, 572–585 (2014).
41. Binnendyk, J. & Pennycook, G. Intuition, reason, and conspiracy beliefs. *Curr. Opin. Psychol.* **47**, 101387 (2022).
42. Corlett, P. R. *et al.* Disrupted prediction-error signal in psychosis: evidence for an associative account of delusions. *Brain J. Neurol.* **130**, 2387–2400 (2007).
43. Corlett, P. R., Frith, C. D. & Fletcher, P. C. From drugs to deprivation: a Bayesian framework for understanding models of psychosis. *Psychopharmacology (Berl.)* **206**, 515–530 (2009).
44. Denève, S. & Jardri, R. Circular inference: mistaken belief, misplaced trust. *Curr. Opin. Behav. Sci.* **11**, 40–48 (2016).
45. McNeish, D. M. & Stapleton, L. M. The effect of small sample size on two-level model estimates: A review and illustration. *Educ. Psychol. Rev.* **28**, 295–314 (2016).
46. Fletcher, R., Cornia, A. & Nielsen, R. K. How Polarized Are Online and Offline News Audiences? A Comparative Analysis of Twelve Countries. *Int. J. Press.* **25**, 169–195 (2020).
47. Boddington, A. Sejanus. Whose Conspiracy? *Am. J. Philol.* **84**, 1–16 (1963).
48. Leptourgos, P., Denève, S. & Jardri, R. Can circular inference relate the neuropathological and behavioral aspects of schizophrenia? *Curr. Opin. Neurobiol.* **46**, 154–161 (2017).
49. Derome, M. *et al.* Functional connectivity and glutamate levels of the medial prefrontal cortex in schizotypy are related to sensory amplification in a probabilistic reasoning task. *NeuroImage* **278**, 120280 (2023).
50. Mamassian, P. & Goutcher, R. Temporal dynamics in bistable perception. *J. Vis.* **5**, 7 (2005).
51. UNESCO Institute for Statistics & Statistics, U. I. for. International Standard Classification of Education (ISCED). http://uis.unesco.org/en/topic/international-standard-classification-education-isced (2020).
52. Brotherton, R., French, C. & Pickering, A. Measuring Belief in Conspiracy Theories: The Generic Conspiracist Beliefs Scale. *Front. Psychol.* **4**, (2013).
53. Lantian, A., Muller, D., Nurra, C. & Douglas, K. M. Measuring Belief in Conspiracy Theories: Validation of a French and English Single-Item Scale. *Int. Rev. Soc. Psychol.* **29**, 1 (2016).
54. Jardri, R. & Denève, S. Circular inferences in schizophrenia. *Brain J. Neurol.* **136**, 3227–3241 (2013).